Inorganic Chemistry

ARTICLE

pubs.acs.org/IC

Structure and Bonding Energy Analysis of Cationic Metal−Ylyne Complexes of Molybdenum and Tungsten, $[(MeCN)(PMe_3)_4M{\equiv}EMes]^+$ (M = Mo, W; E = Si, Ge, Sn, Pb): A Theoretical Study

Krishna K. Pandey,*[,†] Pankaj Patidar,[†] and Philip P. Power[‡,§]

[†]School of Chemical Sciences, Devi Ahilya University Indore, Indore 452 017, India

[‡]Department of Chemistry, University of California, Davis, One Shields Avenue, Davis, California 95616, United States

Supporting Information

ABSTRACT:

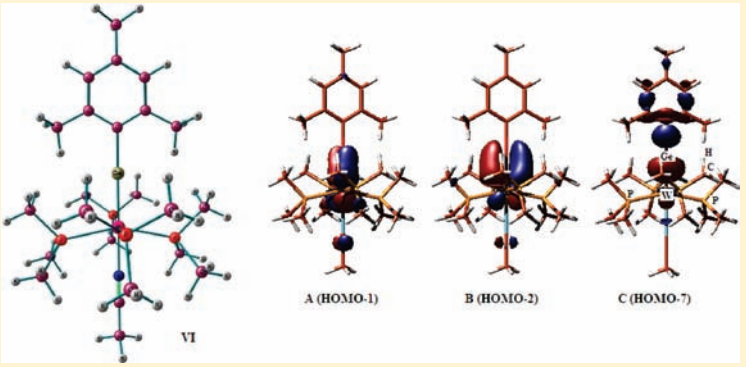

The molecular and electronic structures and bonding analysis of terminal cationic metal−ylyne complexes $(MeCN)(PMe_3)_4M{\equiv}EMes]^+$ (M = Mo, W; E = Si, Ge, Sn, Pb) were investigated using DFT/BP86/TZ2P/ZORA level of theory. The calculated geometrical parameters for the model complexes are in good agreement with the reported experimental values. The M−E σ-bonding orbitals are slightly polarized toward E except in the complex $[(MeCN)(PMe_3)_4W(SnMes)]^+$, where the M−E σ-bonding orbital is slightly polarized toward the W atom. The M−E π-bonding orbitals are highly polarized toward the metal atom. In all complexes, the π-bonding contribution to the total M≡EMes bond is greater than that of the σ-bonding contribution and increases upon going from M = Mo to W. The values of orbital interaction ΔE_{orb} are significantly larger in all studied complexes **I**−**VIII** than the electrostatic interaction ΔE_{elstat}. The absolute values of the interaction energy, as well as the bond dissociation energy, decrease in the order Si > Ge > Sn > Pb, and the tungsten complexes have stronger bonding than the molybdenum complexes.

INTRODUCTION

Since the first report of a carbyne complex in 1973 by Fischer and co-workers,[1] the synthesis, structure, reactivity, and bonding of transition-metal complexes with terminal carbyne (CR) ligands have been a provocative subject and much knowledge of their properties has been obtained.[2−14] In sharp contrast to complexes with carbyne ligands CR, the research on its heavier analogues with ER (E = Si, Ge, Sn, Pb) has been much less developed. The known transition metal−ylyne complexes containing M≡ER bonds can be divided into two classes: (a) terminal neutral metal−ylyne complexes and (b) terminal cationic metal−ylyne complexes. Power and co-workers reported the neutral germylyne complexes of chromium, molybdenum, and tungsten, $[(\eta^5\text{-}C_5H_5)(CO)_2M{\equiv}GeR]$ (M = Cr, Mo, W; R = C_6H_3-2,6-Mes_2, C_6H_3-2,6-$Trip_2$), which are the first representative complexes containing triple bonds to a heavier group 14 element.[15,16] The synthesis, structure, and reactivity of a complex containing a molybdenum−silicon triple bond, $[(\eta^5\text{-}C_5Me_5)(CO)_2Mo{\equiv}SiR]$ (R = 2,6-{2,4,6-$(CMe_2H)_3C_6H_2$}-C_6H_3), have been reported recently by Filippou and co-workers.[17,18] A number of different types of neutral metal−ylyne complexes (see Table 1) have also been reported by the Filippou group.[19−27]

Only five cationic metal−ylyne complexes are reported so far (see Chart 1). Tilley and Mork reported the first example of a transition-metal complex with true silylyne character, $[(\eta^5\text{-}C_5Me_5)(dmpe)(H)Mo{\equiv}SiMes][B(C_6F_5)_4]$ (dmpe = $Me_2PCH_2CH_2PMe_2$);[28] however, it possesses significant interaction between the hydrogen and silicon centers. The previously known compound $[(\eta^5\text{-}C_5Me_5)(Me_3P)_2RuSi\{(bipy)\text{-}(SC_6H_4\text{-}4\text{-}Me)\}][OTf]_2$ can be formally described as a silylyne complex, but it

Received: March 23, 2011
Published: June 23, 2011

Table 1. Experimentally Known Neutral Transition Metal−Ylyne Complexes with M≡E Bonds (M = Cr, Mo, W; E = Si, Ge, Sn, Pb)

complexes[a]	M−E (Å)	E−C (Å)	M−E−C (deg)	ref
$[(\eta^5\text{-}C_5H_5)(CO)_2Mo{\equiv}Ge(R^*)]$	2.272(8)	1.936(5)	174.25(14)	15
$[(\eta^5\text{-}C_5H_5)(CO)_2Cr{\equiv}Ge(R^*)]$	2.1666(4)	1.9512(18)	175.99(6)	16
$[(\eta^5\text{-}C_5H_5)(CO)_2W{\equiv}Ge(R^*)]$				16
$[(\eta^5\text{-}C_5H_5)(CO)_2Mo{\equiv}Ge(R)]$	2.271(1)	1.933(7)	177.2(2)	16
$[(\eta^5\text{-}C_5H_5)(CO)_2W{\equiv}Ge(R)]$	2.2767(14)	1.916(11)	170.9(3)	16
$[(\eta^5\text{-}C_5H_5)\ (CO)_2Mo{\equiv}Si(R^*)]$	2.2241(7)	1.859(2)	173.49(8)	17, 18
$[Cl(dppe)_2W{\equiv}Ge(\eta^1\text{-}C_5Me_5)]$	2.302(1)	2.038(5)	172.2(2)	19
$[Br(dppe)_2W{\equiv}Ge(\eta^1\text{-}C_5Me_5)]$	2.293(1)	2.030(8)	172.4(2)	19
$[I(dppe)_2W{\equiv}Ge(\eta^1\text{-}C_5Me_5)]$	2.3060(9)	2.049(6)	172.6(2)	19
$[Cl(dppe)_2Mo{\equiv}Ge(\eta^1\text{-}C_5Me_5)]$	2.3185(6)	2.049(4)	172.0(1)	20
$[Br(dppe)_2Mo{\equiv}Ge(\eta^1\text{-}C_5Me_5)]$	2.3103(6)	2.029(5)	171.6(2)	20
$[H(dppe)_2W{\equiv}Ge(\eta^1\text{-}C_5Me_5)]$	2.310(1)	2.037(4)	176.8(1)	21
$[(NCO)(dppe)_2W{\equiv}Ge(\eta^1\text{-}C_5Me_5)]$	2.2991(9)	2.031(5)	172.0(1)	21
$[(SCN)(dppe)_2W{\equiv}Ge(\eta^1\text{-}C_5Me_5)]$				21
$[(N_3)(dppe)_2W{\equiv}Ge(\eta^1\text{-}C_5Me_5)]$				21
$[CN(dppe)_2W{\equiv}Ge(\eta^1\text{-}C_5Me_5)]$	2.3184(6)	2.008(4)	172.2(1)	21
$[Cl(depe)_2Mo{\equiv}Ge(\eta^1\text{-}C_5Me_5)]$				22
$[Br(depe)_2Mo{\equiv}Ge(\eta^1\text{-}C_5Me_5)]$	2.2798(5)	2.046(3)	177.46(8)	22
$[Cl(depe)_2W{\equiv}Ge(\eta^1\text{-}C_5Me_5)]$				22
$[Br(depe)_2W{\equiv}Ge(\eta^1\text{-}C_5Me_5)]$				22
$[Cl(PMe_3)_4Mo{\equiv}Ge(R^*)]$				23
$[Cl(PMe_3)_4W{\equiv}Ge(R^*)]$	2.338(1)	1.982(10)	177.9(3)	23
$[I(PMe_3)_4W{\equiv}Ge(R^*)]$	2.3206(4)	2.004(2)	175.79(3)	23
$[(SCN)(PMe_3)_4W{\equiv}Ge(R^*)]$				23
$[H(PMe_3)_4W{\equiv}Ge(R^*)]$	2.324(1)	1.977(6)	178.9(2)	23
$[Cl(PMe_3)_4W{\equiv}Sn(R)]$	2.4901(7)	2.179(5)	178.2(1)	24
$[Cl(dppe)_2W{\equiv}Sn(R)]$				25
$[Br(PMe_3)_4Mo{\equiv}Pb(R^*)]$	2.5495(8)	2.277(7)	177.8(2)	26
$[Br(PMe_3)_4W{\equiv}Pb(R^*)]$	2.5464(5)	2.254(6)	177.5(2)	27
$[I(PMe_3)_4W{\equiv}Pb(R^*)]$	2.5477(3)	2.258(3)	175.79(8)	27
$[H(PMe_3)_4W{\equiv}Pb(R^*)]$	2.5525(3)	2.229(6)	178.7(2)	27

[a] dppe = 1,2-bis(diphenylphosphino)ethane $[1,2\text{-}(Ph_2P)_2C_2H_4]$; depe = 1,2-bis(diphenylphosphino)ethane $[1,2\text{-}\{(C_2H_5\}_2P)_2C_2H_4]$; R = 2,6-bis(2,4,6-trimethylphenyl)phenyl $[2,6\text{-}\{2,4,6\text{-}Me_3C_6H_2\}_2C_6H_3]$; R* = 2,6-bis[2,4,6-tris(2-propyl)phenyl]phenyl $[2,6\text{-}\{2,4,6\text{-}(CMe_2H)_3C_6H_2\}_2C_6H_3]$.

has four-coordinate silicon.[29] Cationic tungsten−ylyne complexes $[(MeCN)(dppe)_2W{\equiv}GeCp^*)]^+$, $[(dppe)_2W{\equiv}SnR]\text{-}[PF_6]$ (R = C_6H_3-2,6-Mes_2), and $[L(PMe_3)_4W{\equiv}PbR)]^+$ (L = PMe_3, PhCN) have been reported by Filippou et al.[21,25,30] The Mössbauer spectral study of stannylyne complexes has also been performed.[31]

The chemical bonding in these complexes can be considered as donor−acceptor orbital interactions, which are schematically presented in Figure 1. The fragments $[EMes]^+$ have a doubly occupied σ orbital, which serves as a donor orbital, and doubly degenerate empty p(π) orbitals, which serve as acceptor orbitals. The π interactions in molecules using C_s symmetry are labeled as in-plane ($\pi_{\|}$) and out-of-plane ($\pi_{\perp}$) π contributions.

A number of previous theoretical approaches have been proven to be an indispensable part of the studies of the linear M≡E (E = Si, Ge, Sn, Pb) bonds.[19,24−26,32,33] We have reported the differences between the chemical-bonding situations of metal−ylyne complexes and metalloylenes.[34,35] We decided to investigate the chemical bonding in the cationic metal−ylyne complexes of molybdenum and tungsten, $[(MeCN)(PMe_3)_4\text{-}M{\equiv}EMes]^+$, with energy decomposition analysis. It has been shown that the results give quantitative insight into the nature of the metal−ligand interactions.[34−40]

In this paper, we report the geometry and electronic structure as well as the nature of M≡E bonds in the cationic transition-metal silylyne, germylyne, stannylyne, and plumbylyne complexes $[(MeCN)(PMe_3)_4Mo{\equiv}EMes]^+$ (**I**, E = Si; **II**, E = Ge; **III**, E = Sn; **IV**, E = Pb) and $[(MeCN)(PMe_3)_4W{\equiv}EMes]^+$ (**V**, E = Si; **VI**, E = Ge; **VII**, E = Sn; **VIII**, E = Pb) at the DFT/BP86/TZ2P level of theory. Bonding analysis for the cationic plumbylyne complex $[(PMe_3)_5W{\equiv}PbR)]^+$ [R = 2,6-bis(2,4,6-trimethylphenyl)phenyl] has been investigated.[30] The complexes **I**−**VIII** serve as models for the structures **B**−**E** (Chart 1). In the model complexes, the bulky substituents at the Si, Ge, Sn, and Pb atoms are replaced by a mesityl group, 2,4,6-$(CH_3)_3C_6H_2$. The main goals of the present study are (i) to investigate the optimized structures of the model complexes, (ii) to analyze the nature of the M≡E bonds of the metal−ylyne complexes, (III) to investigate the degree of ionic and covalent character of the M≡E bond, and (iv) to study the extent of the M ← E σ-bonding and M → E π-back-bonding contribution to the M≡E bonds. The present study reports for the first time a comprehensive

dx.doi.org/10.1021/ic2005908 |Inorg. Chem. 2011, 50, 7080–7089

Chart 1. Experimentally Known Cationic Transition Metal−Ylyne Complexes[a]

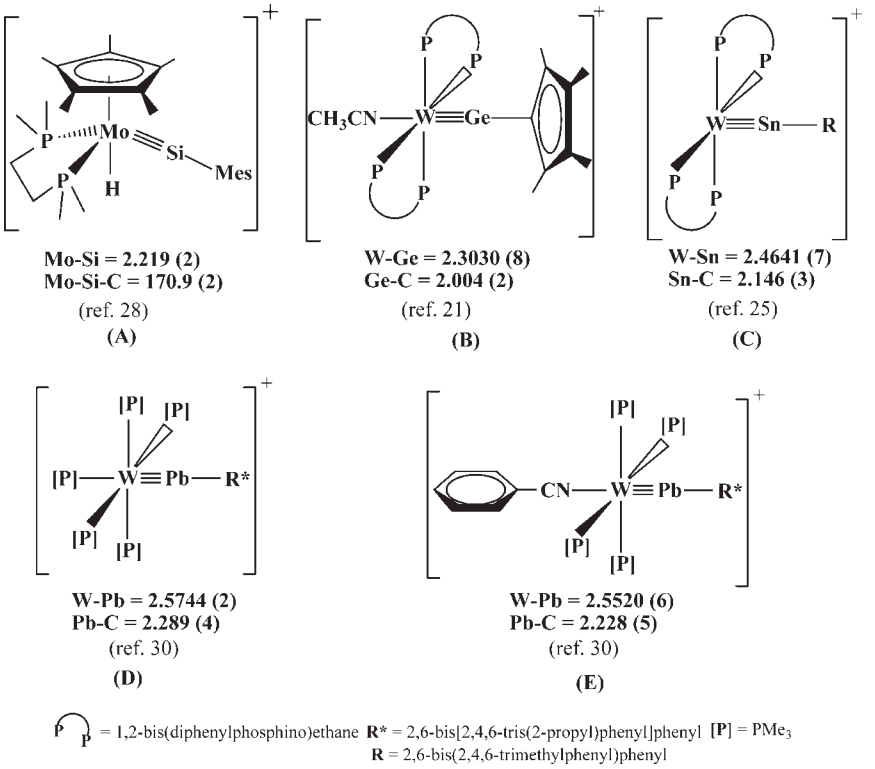

[a]The bond lengths are in angstroms, and the bond angles are in degrees.

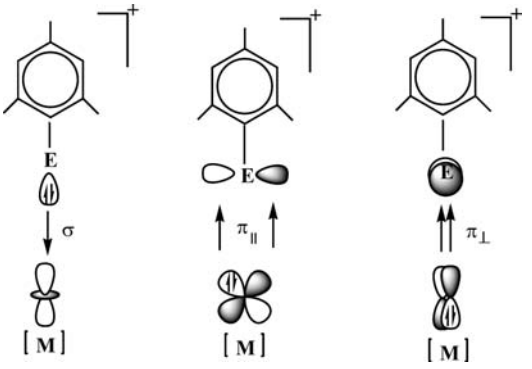

Figure 1. Schematic representation of the orbital interaction between closed-shell metal fragments [M] and group 14 ligand fragments $[EMes]^+$.

theoretical investigation of a complete series of cationic transition metal−ylyne complexes **I**−**VIII**.

COMPUTATIONAL METHODS

The geometries of all complexes have been optimized at the gradient-corrected density functional theory (DFT) level of theory using the exchange functional of Becke[41] in conjunction with the correlation functional of Perdew[42,43] (BP86). Uncontracted Slater-type orbitals (STOs) were employed as basis functions for the self-consistent-field (SCF) calculations.[44] The basis sets have triple ξ quality augmented by two sets of polarization functions. The $(n-1)s^2$ and $(n-1)p^6$ core electrons of the main-group elements, the $(1s2s2p3s3p3d)^{28}$ core electrons of molybdenum, and the $(1s2s2p3s3p3d4s4p4d)^{46}$ core

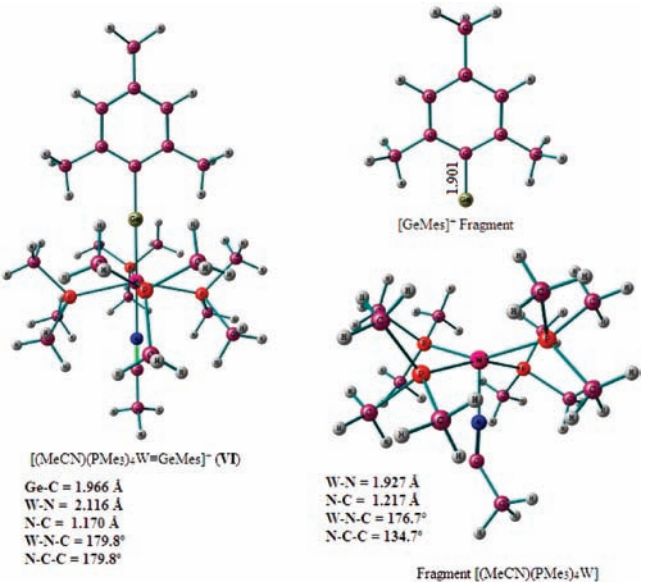

Figure 2. Optimized structure of the tungsten−germylyne complex cation $[(MeCN)(PMe_3)_4W{\equiv}GeMes]^+$ (**VI**) and its interacting fragments $[(MeCN)(PMe_3)_4W]$ and $[GeMes]^+$. Important bond distances and angles for complexes **I**−**VIII** are given in Table 2.

electrons of tungsten were treated by the frozen-core approximation.[45] This level of theory is denoted as BP86/TZ2P. An auxiliary set of s, p, d, f, and g STOs was used to fit the molecular densities and to represent the Coulomb and exchange potentials accurately in each SCF cycle.[46] Scalar relativistic effects have been considered using the zero-order regular

dx.doi.org/10.1021/ic2005908 |*Inorg. Chem.* 2011, 50, 7080–7089

approximation (ZORA).[47−52] The calculations were carried out with the program package *ADF 2009.01*.[53]

Table 2. Selected Optimized Structural Parameters[a] for Cationic Transition Metal−Ylyne Complexes $[(MeCN)(PMe_3)_4M{\equiv}EMes]^+$ (M = Mo, W; E = Si, Ge, Sn, Pb) at the BP86/TZ2P Level

	Mo				W			
	Si	Ge	Sn	Pb	Si	Ge	Sn	Pb
				Bond Distances				
M≡E	2.272	2.312	2.511	2.571	2.297	2.332	2.532	2.589
E−C	1.884	1.967	2.161	2.244	1.884	1.966	2.160	2.243
M−N	2.151	2.139	2.112	2.099	2.129	2.116	2.093	2.080
C−N	1.167	1.168	1.169	1.171	1.169	1.170	1.171	1.173
				Bond Angles				
M−E−C	179.8	179.9	179.2	179.1	179.1	179.8	179.5	179.4
N−M−E	179.8	179.7	179.7	179.7	179.4	179.9	179.8	179.8
E−M−P (in)	86.2	85.9	86.6	86.9	85.9	85.8	86.4	86.7
E−M−P (out)	102.3	101.6	101.0	100.7	102.3	101.6	100.8	100.4

[a] Distances are in angstroms, and angles are in degrees.

The bonding interactions between the metal fragment [(MeCN)-$(PMe_3)_4$Mo] or [(MeCN)$(PMe_3)_4$W] and ligand fragments $[EMes]^+$ (singlet states) have been analyzed with the energy decomposition scheme of the program package ADF, which is based on the work by Morokuma[54] and Ziegler and Rauk.[55] The bond dissociation energy (BDE) between the fragments is partitioned into several contributions that can be identified as physically meaningful quantities. First, ΔE is separated into two major components, ΔE_{int} and ΔE_{prep}:

$$\Delta E = \Delta E_{int} + \Delta E_{prep} \quad (1)$$

ΔE_{prep} is the energy that is necessary to promote the fragments from their equilibrium geometry and electronic ground state to the geometry, and electronic state, that they have in the molecule. The instantaneous interaction energy ΔE_{int} is the focus of the bonding analysis and can be decomposed into three components:

$$\Delta E_{int} = \Delta E_{elstat} + \Delta E_{Pauli} + \Delta E_{orb} \quad (2)$$

The term ΔE_{elstat} gives the electrostatic interaction energy between the fragments that are calculated with a frozen density distribution in the geometry of the complex. The term ΔE_{Pauli}, which is called the exchange or Pauli repulsion, takes into account the destabilizing two-orbital three- or four-electron interactions between occupied orbitals of both fragments. ΔE_{Pauli} is calculated by forcing the Kohn−Sham determinant of the molecule, which results from superimposing both fragments, to obey

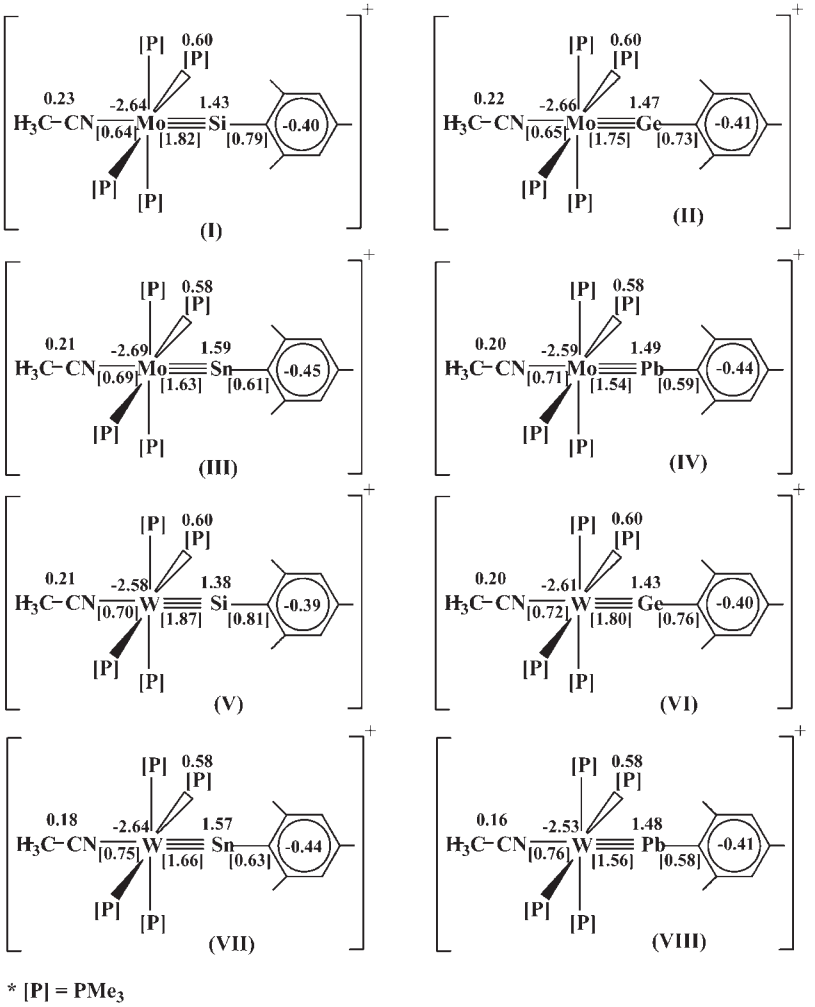

Figure 3. NPA charge distributions in cationic transition metal−ylyne complexes $[(MeCN)(PMe_3)_4M{\equiv}EMes]^+$ (M = Mo, W; E = Si, Ge, Sn, Pb) (**I**−**VIII**). The values in parentheses are the WBIs.

dx.doi.org/10.1021/ic2005908 |*Inorg. Chem.* 2011, 50, 7080–7089

Table 3. Results of NBO Analysis in Cationic Transition Metal−Ylyne Complexes $[(MeCN)(PMe_3)_4M{\equiv}EMes]^+$ (M = Mo, W; E = Si, Ge, Sn, Pb)

	Mo				W			
	Si (**I**)	Ge (**II**)	Sn (**III**)	Pb (**IV**)	Si (**V**)	Ge (**VI**)	Sn (**VII**)	Pb (**VIII**)
				M≡E σ Bonds				
occupancy	1.815	1.801	1.757	1.715	1.850	1.835	1.789	1.746
M								
%	48.65	48.20	49.26	44.48	49.29	49.15	51.09	46.36
% s	32.11	30.61	29.16	26.72	31.74	30.27	28.51	25.90
% p	31.31	32.77	36.42	37.66	30.83	32.04	35.16	35.89
% d	36.56	36.61	34.42	35.61	37.42	37.67	36.33	38.20
% f	0.02	0.01	0.00	0.01	0.01	0.02	0.00	0.01
E								
%	51.35	51.80	50.54	55.52	50.71	50.85	48.91	53.64
% s	63.89	63.70	62.50	61.45	63.36	63.20	61.90	61.17
% p	36.10	36.29	37.45	38.38	36.63	36.80	38.05	38.68
% d	0.01	0.01	0.05	0.17	0.01	0.00	0.05	0.15
				M≡E π Bonds				
occupancy	1.798	1.791	1.777	1.769	1.790	1.783	1.762	1.751
M								
%	74.61	76.59	79.22	80.56	73.12	75.35	78.34	79.87
% p	14.70	14.41	12.83	11.78	13.55	13.15	11.56	10.45
% d	85.30	85.59	87.17	88.22	86.45	86.85	88.44	89.55
E								
%	25.39	23.41	20.78	19.44	26.88	24.65	21.66	20.13
% p	99.77	99.93	99.93	99.72	99.80	99.94	99.94	99.74
% d	0.23	0.07	0.07	0.28	0.20	0.06	0.06	0.26
occupancy	1.805	1.800	1.786	1.781	1.771	1.764	1.745	1.737
M								
%	79.10	80.53	82.21	83.25	77.62	79.18	81.08	82.21
% p	2.49	2.28	1.68	1.46	1.54	1.36	0.92	0.75
% d	97.51	97.72	98.32	98.54	98.46	98.64	99.08	99.25
E								
%	20.90	19.47	17.79	16.75	22.38	20.82	18.92	17.79
% p	99.70	99.88	99.96	99.75	99.73	99.89	99.97	99.79
% d	0.30	0.12	0.04	0.25	0.27	0.11	0.03	0.21

the Pauli principle through antisymmetrization and renormalization. The last term ΔE_{orb} in eq 1 gives the stabilizing orbital interactions between the occupied and virtual orbitals of the two fragments. ΔE_{orb} can be further partitioned into contributions by the orbitals that belong to different irreducible representations of the point group of the system. It has been suggested that the covalent and electrostatic character of a bond is given by the ratio $\Delta E_{elstat}/\Delta E_{orb}$. The electronic structures of the complexes **I**−**VIII** were examined by natural bond order (NBO) analysis.[56] The molecular orbitals were made by using the *MOLDEN* program.[57]

RESULTS AND DISCUSSION

Geometries. Figure 2 displays the representative optimized geometries of the cationic tungsten−germylyne complex **VI** and its fragments $[(MeCN)(PMe_3)_4W]$ and $[GeMes]^+$. The structures of silylyne, stannylyne, and plumbylyne complexes are very similar to those presented in this figure and are therefore not included. The important bond distances and angles of the eight cationic complexes $[(MeCN)(PMe_3)_4Mo{\equiv}EMes]^+$ (**I**, E = Si; **II**, E = Ge; **III**, E = Sn; **IV**, E = Pb), and $[(MeCN)(PMe_3)_4W{\equiv}EMes]^+$ (**V**, E = Si; **VI**, E = Ge; **VII**, E = Sn; **VIII**, E = Pb) calculated at the BP86/TZ2P level of theory are represented in Table 2. The important optimized geometrical parameters of the molybdenum fragment $[(MeCN)(PMe_3)_4Mo]$ are Mo−N = 1.943 Å, N−C = 1.207 Å, M−N−C = 176.1°, and N−C−C = 142.6° and the ligand fragments $[EMes]^+$ are Si−C = 1.802 Å, Ge−C = 1.901 Å, Sn−C = 2.110 Å, and Pb−C = 2.205 Å.

The optimized M≡E bond distances in the cationic complexes **I**−**VIII** are in good agreement with the experimental values reported for metal−ylyne complexes (see Table 2 and Chart 1). We observe a steady increase of the M≡E bond distances on going from molybdenum to tungsten, which further increases upon descending group 14 (**I**, Mo−Si, 2.272 Å; **II**, Mo−Ge, 2.312 Å; **III**, Mo−Sn, 2.511 Å; **IV**, Mo−Pb, 2.571 Å; **V**, W−Si,

dx.doi.org/10.1021/ic2005908 |*Inorg. Chem.* 2011, 50, 7080–7089

Table 4. Energy Decomposition Analysis[a] for Cationic Transition Metal−Ylyne Complexes $[(MeCN)(PMe_3)_4M{\equiv}EMes]^+$ (M = Mo, W; E = Si, Ge, Sn, Pb) at the BP86/TZ2P Level[b]

	Mo				W			
	Si (**I**)	Ge (**II**)	Sn (**III**)	Pb (**IV**)	Si (**V**)	Ge (**VI**)	Sn (**VII**)	Pb (**VIII**)
ΔE_{pauli}	125.1	115.1	94.6	89.3	136.1	126.7	104.2	99.4 [112.8][c]
ΔE_{int}	−129.9	−123.9	−108.4	−97.8	−138.2	−131.8	−115.3	−103.9 [−98.2][c]
ΔE_{elstat}	−94.2	−85.9	−75.5	−70.6	−104.7	−96.1	−83.8	−78.7 [−84.1][c]
ΔE_{orb}[d]	−160.8 (63.1)	−153.2 (64.1)	−127.5 (62.8)	−116.6 (62.3)	−169.7 (61.8)	−162.5 (62.8)	−135.7 (61.8)	−124.6 [−126.9][c] (61.3)
$\Delta E_{a'}$	−90.1	−86.0	−72.9	−66.9	−96.2	−92.3	−78.8	−72.7
$\Delta E_{a''}$	−70.7	−67.2	−54.6	−49.7	−73.5	−70.2	−56.9	−51.9
% π_{out}[e]	{43.9}	{43.9}	{42.8}	{42.7}	{43.3}	{43.2}	{41.9}	{41.7}
ΔE_{prep}	14.6	12.9	10.6	9.8	17.1	15.3	12.8	11.8
ΔE (−De)	−115.3	−111.0	−97.8	−88.0	−121.1	−116.6	−102.4	−92.1

[a] Energy contribution in kcal/mol. [b] $[(MeCN)(PMe_3)_4W]$ and $[EMes]^+$ fragments have been considered. [c] The values in square brackets are previously calculated values for the W≡Pb bond in the complex $[(PMe_3)_5W{\equiv}Pb(2,6\text{-}Trip_2C_6H_3]^+]$ considering $[(PMe_3)_5W]$ and $[Pb(2,6\text{-}Trip_2C_6H_3]^+$ fragments.[30] [d] The values in parentheses are the percentage contribution to the total attractive interactions reflecting the total covalent character of the bond. [e] The values in the parentheses are the percentage π-character contribution in the total orbital interaction, ΔE_{orb}.

2.297 Å; **VI**, W−Ge, 2.332 Å; **VII**, W−Sn, 2.532 Å; **VIII**, W−Pb, 2.589 Å). The M≡E bond distances in complexes **I**−**VIII** are significantly shorter than those expected from single-bond covalent radii predictions (Mo−Si = 2.58 Å, Mo−Ge = 2.62 Å, Mo−Sn = 2.80 Å, and Mo−Pb = 2.87 Å; W−Si = 2.59 Å, W−Ge = 2.63 Å, W−Sn = 2.81 Å, and W−Pb = 2.88 Å).[58]

The optimized E−C bond distances in complexes **I**−**VIII** (Table 2) are slightly shorter than those expected for a single bond based on covalent radii (Si−C = 1.95 Å, Ge−C = 1.99 Å, Sn−C = 2.17 Å, and Pb−C = 2.24 Å). The shortening of the E−C bonds may be due to weak E−C(Mes) π bonding. The M−N (M = Mo, W) bond distances in complexes **I**−**VIII** are also shorter than those expected for a single bond based on covalent radii (Mo−N = 2.15 Å and W−N = 2.16 Å). The results reveal strong M−N bonding in the studied complexes. From silicon to lead, the M−N bond strength increases. The M−E−C and N−M−E bond angles are almost linear (>179°) in all of the studied complexes. Moreover, the P−M−E bond angles with out-of-plane P atoms are wider than the in-plane P−M−E bond angles.

Bonding Analysis of M≡E Bonds. The electronic structures of complexes **I**−**VIII** were analyzed with a discussion of the conventional indices that are frequently used to characterize the bonding in molecules, that is, bond orders and atomic charges. Figure 2 gives the Wiberg bond indices (WBIs)[59] and the natural population analysis (NPA) charge distributions.

As seen in Figure 3, the WBI values of the M−E bonds in complexes **I**−**VIII** are significantly higher (1.54−1.87), indicating a substantial degree of multiple M−E bonding. Like the M≡E bond distances, upon going from Mo to W, the WBI values of the M≡E bonds increase as 1.82 (**I**) < 1.87 (**V**), 1.75 (**II**) < 1.80 (**VI**), 1.63 (**III**) < 1.66 (**VII**), 1.54 (**IV**) < 1.56 (**VIII**). We also found decreases in the WBI values of M≡E upon going from silylyne to plumbylyne ligands. The WBIs of the E−C(Mes) bonds decrease on going from E = Si to Pb in both sets of complexes (Figure 3). The trends are consistent with those reported above for the calculated geometries.

The calculated charge distribution indicates that the metal atoms always carry a negative charge while the heavier group 14 elements (E) and EMes ligands are positively charged. It is important to note that the NBO analysis generally gives high values of NPA charges (see Table S1 in the Supporting Information).[60] The charges on the E atoms vary as Si < Ge < Sn > Pb. The acetonitrile and PMe_3 ligands are positively charged, while the Mes ring carries a negative charge (Figure 3).

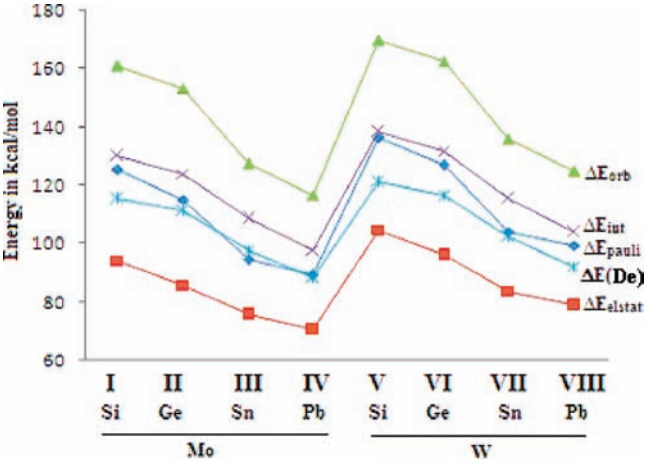

Figure 4. Trends of the absolute values of the interaction energy, orbital interactions (covalent contributions), electrostatic interacton (ionic contributions), Pauli repulsive interaction, and bond dissociation energy (De) to the M≡E bond in the cationic metal−ylyne complexes $[(MeCN)(PMe_3)_4M{\equiv}EMes]^+$ (M = Mo, W; E = Si, Ge, Sn, Pb; **I**−**VIII**).

A more definitive picture of M≡E bonding is obtained through NBO analysis of the delocalized Kohn−Sham orbitals. The characteristics of the M≡E one σ component (a′ symmetry) and two nearly degenerate π components (in-plane and out-of-plane with a′ and a″ symmetry, respectively) are listed in Table 3. In most of the complexes **I**−**VIII**, the M−E σ-bonding orbital is slightly polarized toward the heavier group 14 elements (i.e., the E atom contributes more to the bonding orbital) except complex $[(MeCN)(PMe_3)_4W{\equiv}SnMes]^+$, where the M−E σ-bonding orbital is slightly polarized toward the metal atom. The occupations for M−E σ-bonding orbitals are in the range 1.746−1.850. In both sets of metal−ylyne complexes of molybdenum and

dx.doi.org/10.1021/ic2005908 |*Inorg. Chem.* 2011, 50, 7080–7089

tungsten, **I**−**VIII**, the M−E π-bonding orbitals are highly polarized toward the metal atom (i.e., the metal center contributes significantly more to the bonding orbital). The contributions of E to the π bonding are small (Table 3).

Energy Decomposition Analysis of M≡E Bonds. To quantify the above information and to obtain more detailed insight into the nature of the M≡E interactions, we carried out an energy decomposition analysis of complexes **I**−**VIII**. The results are given in Table 4 and Figure 4. The charge on the EMes ligands is significantly positive, with values ranging from +0.99 to +1.16. For this reason, we considered $[(MeCN)(PMe_3)_4M]$ and $[EMes]^+$ fragments in the decomposition analysis.

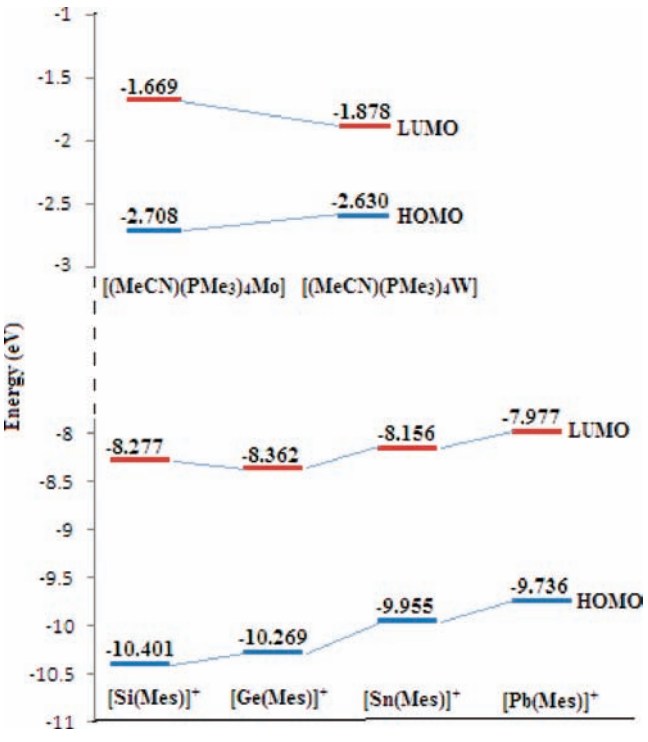

Figure 5. HOMOs and LUMOs of Kohn−Sham molecular orbitals of fragments $[(MeCN)(PMe_3)_4M]$ (M = Mo, W) and $[EMes]^+$ (E = Si, Ge, Sn, Pb).

The calculated data in Table 4 show that the M≡EMes bonds in cationic complexes $[(MeCN)(PMe_3)_4M{\equiv}EMes]^+$ (**I**−**VIII**) are rather strong. The magnitude of the energy terms slightly decreases in the order W > Mo as coordinating metal. The tabulated results for tungsten reveal the expected periodic trend in the bond strengths due to the d-orbital extent: the W≡E bonds are stronger than the corresponding Mo≡E bonds. BDEs decrease on going from silylyne to plumbylyne complexes. We note a steady decrease in the BDEs. The nature and properties of the highest occupied (HOMOs) and lowest unoccupied (LUMOs) molecular orbitals of the fragments $[(MeCN)(PMe_3)_4M]$ and $[EMes]^+$ (Figure 5) play a important role in explaining the orbital interaction differences. The LUMO of $[GeMes]^+$ (87.21% Ge; 8.85% Mes) has relatively more contribution of Mes than the LUMO of $[SiMes]^+$ (87.02% Si; 8.11% Mes), and hence it is more stabilized. The difference in energy of the HOMO orbitals of the fragments $[(MeCN)(PMe_3)_4M]$ on going from molybdenum to tungsten may be due to the relativistic changes in energies of the tungsten-based d orbitals. The energy increase for the HOMO of the tungsten fragment $[(MeCN)(PMe_3)_4W]$ will enhance $[(MeCN)(PMe_3)_4W] \rightarrow [EMes]^+$ π back-donation because this orbital is closer to the LUMO of $[EMes]^+$ fragments. Also, the energy decrease for the LUMO of $[(MeCN)(PMe_3)_4W]$ will enhance $[(MeCN)(PMe_3)_4M] \leftarrow [EMes]^+$ σ donation. Thus, the values of the interaction energy as well as BDE are greater for tungsten complexes **V**−**VIII** than those for molybdenum complexes **I**−**IV**.

The breakdown of the interaction energies, ΔE_{int}, into the repulsive term ΔE_{pauli} and the attractive interactions ΔE_{orb} and ΔE_{elstat} shows that the M≡E bonds have greater orbital interaction than electrostatic (ionic) interaction. Table 4 also gives a

Table 5. Comparison of Various Bonding Parameters of the M−E Bond in Previously Reported Metal−Ylyne Complexes $[(\eta^5\text{-}C_5H_5)(CO)_2M{\equiv}EMe]$[a] and Presently Studied Cationic Complexes $[(MeCN)(PMe_3)_4M{\equiv}EMes]^+$[b] (M = Mo, W; E = Si, Ge, Sn, Pb)

complex	M−E bond distance (Å)	ΔE_{elstat}	ΔE_{int}	BDE	ref
$[(\eta^5\text{-}C_5H_5)(CO)_2Mo{\equiv}SiMe]$	2.229	−168.1	−220.9	−211.0	35
$[(MeCN)(PMe_3)_4Mo{\equiv}SiMes]^+$	2.272	−94.2	−129.9	−115.3	this work
$[(\eta^5\text{-}C_5H_5)(CO)_2Mo{\equiv}GeMe]$	2.286	−160.8	−210.5	−204.7	34
$[(MeCN)(PMe_3)_4Mo{\equiv}GeMes]^+$	2.312	−85.9	−123.9	−111.0	this work
$[(\eta^5\text{-}C_5H_5)(CO)_2Mo{\equiv}SnMe]$	2.482	−153.5	−193.6	−185.7	35
$[(MeCN)(PMe_3)_4Mo{\equiv}SnMes]^+$	2.511	−75.5	−108.4	−97.8	this work
$[(\eta^5\text{-}C_5H_5)(CO)_2Mo{\equiv}PbMe]$	2.522	−153.0	−180.3	−172.9	35
$[(MeCN)(PMe_3)_4Mo{\equiv}PbMes]^+$	2.571	−70.6	−97.8	−88.0	this work
$[(\eta^5\text{-}C_5H_5)(CO)_2W{\equiv}SiMe]$	2.239	−180.7	−231.0	−220.1	35
$[(MeCN)(PMe_3)_4W{\equiv}SiMes]^+$	2.297	−104.7	−138.2	−121.1	this work
$[(\eta^5\text{-}C_5H_5)(CO)_2W{\equiv}GeMe]$	2.293	−168.9	−220.6	−213.2	34
$[(MeCN)(PMe_3)_4W{\equiv}GeMes]^+$	2.332	−96.1	−131.8	−116.6	this work
$[(\eta^5\text{-}C_5H_5)(CO)_2W{\equiv}SnMe]$	2.483	−162.8	−202.0	−193.3	35
$[(MeCN)(PMe_3)_4W{\equiv}SnMes]^+$	2.532	−83.8	−115.3	−102.4	this work
$[(\eta^5\text{-}C_5H_5)(CO)_2W{\equiv}PbMe]$	2.521	−163.8	−187.9	−179.9	35
$[(MeCN)(PMe_3)_4W{\equiv}PbMes]^+$	2.589	−78.7	−103.9	−92.1	this work

[a] Fragments $[(\eta^5\text{-}C_5H_5)(CO)_2M]^-$ and $[EMe]^+$. [b] Fragments $[(MeCN)(PMe_3)_4M]$ and $[EMes]^+$.

dx.doi.org/10.1021/ic2005908 |*Inorg. Chem.* 2011, 50, 7080–7089

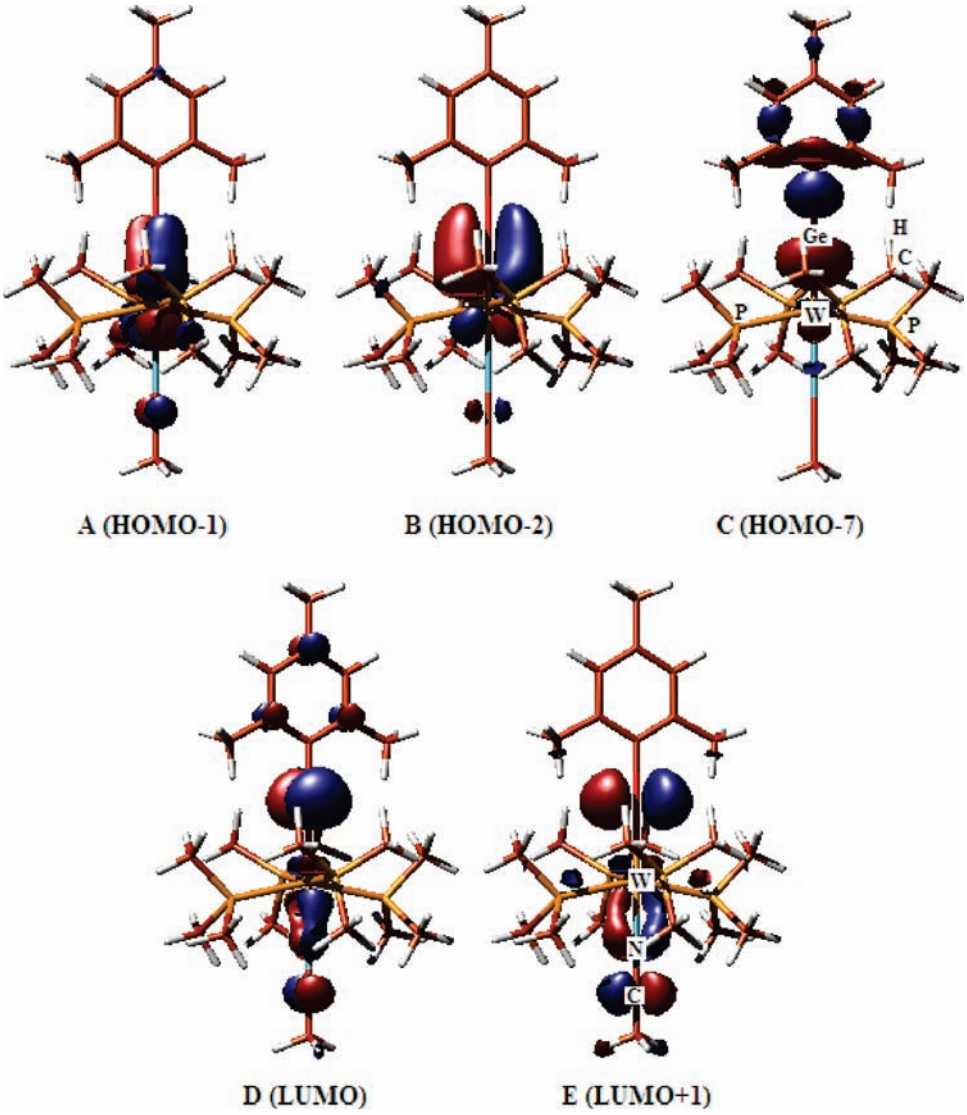

Figure 6. Plot of some relevant molecular orbitals of cationic tungsten−germylyne complex **VI**.

breakdown of the orbital interaction into M ← E σ donation and M → E π back-donation. The covalent bonding has a high degree of π character. We want to emphasis that the calculated energy contribution ΔE_{π} gives only the out-of-plane ($\pi_{\perp}$) component of the [M] → [EMes]$^+$ π back-donation. This is because the molecules have C_s symmetry and the orbitals can only have a′ (σ) and a″ (π) symmetry. Thus, the energy contributions of the a′ orbitals comes from the [M] ← [EMes]$^+$ σ donation but also from the in-plane [M] → [EMes]$^+$ π back-donation. For the molecules that have C_s symmetry, it is not possible to separate the latter two interactions. The energy analysis suggests that, in the complexes **I**−**VIII**, ∼43% of ΔE_{orb} comes from out-of-plane (a″) π bonding. As mentioned earlier, both π bonds are nearly degenerate, and the total π contribution is approximately 80% of the total orbital contribution. On going from silicon to lead, the absolute values of the all energy terms decrease (see Figure 4).

Table 5 shows the M≡E bond distances as well as the bonding energy terms, electrostatic interaction, interaction energy, and BDE of the metal−ylyne complexes [(η^5-C_5H_5)(CO)$_2$M≡EMe] and [(MeCN)(PMe$_3$)$_4$M≡EMes]$^+$ (M = Mo, W; E = Si, Ge, Sn, Pb). We found that the M≡E bonds are relatively longer in the cationic complexes (this work) than those in the neutral metal−ylyne complexes,[34,35] indicating the weakening of M≡E bonds in cationic complexes. As expected, the electrostatic interaction between metal fragments [(MeCN)(PMe$_3$)$_4$M] and [EMes]$^+$ is significantly smaller than that between the fragments [(η^5-C_5H_5)(CO)$_2$M]$^-$ and [EMe]$^+$. Hence, the BDEs as well as interaction energies are also smaller for cationic complexes than for neutral metal−ylyne complexes of molybdenum and tungsten. It is worth mentioning that the BDEs for the neutral complexes [(η^5-C_5H_5)(CO)$_2$M≡EMe] are calculated for the ionic fragments [(η^5-C_5H_5)(CO)$_2$M]$^-$ and [EMe]$^+$.[34,35] Thus, the cationic complexes (**I**−**VIII**) have relatively weaker M≡E bonds.

The strong triple-bond character of the M≡E bonds becomes visible by the envelope plots of some relevant σ and π orbitals of the tungsten−germylyne complex [(MeCN)(PMe$_3$)$_4$W≡GeMes]$^+$ (**VI**; Figure 6).

Parts a (HOMO−1) and b (HOMO−2) of Figure 6 give pictorial descriptions of the W≡Ge π bonding in complex **VI**. The HOMO−1 has a′ symmetry, and HOMO−2 can clearly be identified as having a″ (π) symmetry; however, the shape of the orbital shows clearly that the HOMO−1 has an in-plane π

dx.doi.org/10.1021/ic2005908 |*Inorg. Chem.* 2011, 50, 7080–7089

component of π back-donation. Part c (HOMO−7) of Figure 6 shows mainly W≡Ge σ-bonding orbitals. Parts d (LUMO) and e (LUMO+1) of Figure 6 mainly depict a nonbonding p orbital of Ge atoms but W−N in-plane and out-of-plane π bonding also appear. It becomes clear from Figure 6 that the $[(MeCN)(PMe_3)_4M{\equiv}EMes]^+$ species has a large contribution from π-bonding orbitals.

SUMMARY AND CONCLUSION

From the above-presented theoretical studies of the structure and bonding in cationic metal−ylyne complexes of molybdenum and tungsten, $[(MeCN)(PMe_3)_4M{\equiv}EMes]^+$ (M = Mo, W; E = Si, Ge, Sn, Pb), the following conclusions may be drawn:

1 Here, we reported the geometry and electronic structure as well as analyzed the nature of the M≡EMes bonds in the terminal cationic metal−ylyne complexes of molybdenum and tungsten, **I**−**VIII**. The calculated geometries are in excellent agreement with the experimental values (Chart 1).
2 The M−E bonds in these complexes are nearly M≡E triple bonds. The M−E σ-bonding orbital is slightly polarized toward the E center, except the complex $[(MeCN)(PMe_3)_4W(SnMes)]^+$, where the M−E σ-bonding orbital is slightly polarized toward the metal atom. The M−E π-bonding orbitals are highly polarized toward the metal atom. In all studied complexes, the π-bonding contribution to the total M≡EMes bond is greater than that of σ bonding and increases on going from M = Mo to W.
3 The contributions of the orbital interactions ΔE_{orb} are significantly larger in all studied complexes **I**−**VIII** than the electrostatic contributions ΔE_{elstat}.
4 The absolute values of the interaction energies, as well as BDEs, decrease in the order Si > Ge > Sn > Pb. Moreover, the tungsten complexes are stronger than the molybdenum complexes.

ASSOCIATED CONTENT

Supporting Information. Cartesian coordinates of the optimized geometries of the cationic complexes **I**−**VIII** and data for Hirshfeld, Voronoi deformation density, and NPA charges. This material is available free of charge via the Internet at http://pubs.acs.org.

AUTHOR INFORMATION

Corresponding Authors

*E-mail: kkpandey.schem@dauniv.ac.in
§E-mail: pppower@ucdavis.edu.

ACKNOWLEDGMENT

P.P. thanks the Council of Scientific and Industrial Research and University Grant Commission, New Delhi, India, for generous financial support.

REFERENCES

(1) Fischer, E. O.; Kreis, G.; Kreiter, C. G.; Mueller, J.; Huttner, G.; Lorenz, H. *Angew. Chem., Int. Ed.* **1973**, *12*, 564.
(2) Nugent, W. A.; Mayer, J. M. *Metal−Ligand Multiple Bond*; Wiley: New York, 1988.
(3) Fischer, H.; Hofmann, P.; Kreisel, F. R.; Schrock, R. R.; Schubert, U.; Weiss, K. *Carbyne Complexes*; VCH: New York, 1988.
(4) *Transition-Metal Carbyne Complexes*; Kreisel, F. R., Ed.; Kluwer: Dordrecht, The Netherlands, 1993.
(5) Frenking, G.; Fröhlich, N. *Chem. Rev.* **2000**, *100*, 717.
(6) Choi, S. K.; Gal, Y. S.; Jin, S. H.; Kim, H. K. *Chem. Rev.* **2000**, *100*, 1645.
(7) Cotton, F. A.; Wilkinson, G.; Murillo, C. A.; Bochmann, M. *Advanced Inorganic Chemistry*, 6th ed.; Wiley: New York, 1999.
(8) Schrock, R. R. *Chem. Rev.* **2002**, *102*, 145–179.
(9) Herndon, J. W. *Coord. Chem. Rev.* **2006**, *250*, 1889.
(10) Da Re, R. E.; Hopkins, M. D. *Coord. Chem. Rev.* **2005**, *249*, 1396.
(11) Mindiola, D. J. *Acc. Chem. Res.* **2006**, *39*, 813–821.
(12) Cordiner, R. L.; Gugger, P. A.; Hill, A. F.; Willis, A. C. *Organometallics* **2009**, *28*, 6632.
(13) Colebatch, A. L.; Hill, A. F.; Shang, R.; Willis, A. C. *Organometallics* **2010**, *29*, 6482.
(14) Cordiner, R. L.; Hill, A. F.; Shang, R.; Willis, A. C. *Organometallics* **2011**, *30*, 139.
(15) Simons, R. S.; Power, P. P. *J. Am. Chem. Soc.* **1996**, *118*, 11966.
(16) Pu, L.; Twamley, B.; Haubrich, S. T.; Olmstead, M. M.; Mork, B. V.; Simons, R. S.; Power, P. P. *J. Am. Chem. Soc.* **2000**, *122*, 650.
(17) Filippou, A. C.; Chernov, O.; Stumpf, K. W.; Schnakenburg, G. *Angew. Chem., Int. Ed.* **2010**, *49*, 3296–3300.
(18) Filippou, A. C.; Chernov, O.; Schnakenburg, G. *Angew. Chem., Int. Ed.* **2011**, *50*, 1122–1126.
(19) Filippou, A. C.; Philippopoulos, A. I.; Portius, P.; Neumann, D. U. *Angew. Chem., Int. Ed.* **2000**, *39*, 2778.
(20) Filippou, A. C.; Portius, P.; Philippopoulos, A. I. *Organometallics* **2002**, *21*, 653.
(21) Filippou, A. C.; Philippopoulos, A. I.; Portius, P.; Schnakenburg, G. *Organometallics* **2004**, *23*, 4503.
(22) Filippou, A. C.; Schnakenburg, G.; Philippopoulos, A. I.; Weidemann, N. *Angew. Chem., Int. Ed.* **2005**, *44*, 5979.
(23) Filippou, A. C.; Weidemann, N.; Philippopoulos, A. I.; Schnakenburg, G. *Angew. Chem. Int. Ed.* **2006**, *45*, 5987.
(24) Filippou, A. C.; Portius, P.; Philippopoulos, A. I.; Rohde, H. *Angew. Chem., Int. Ed.* **2003**, *42*, 445.
(25) Filippou, A. C.; Philippopoulos, A. I.; Schnakenburg, G. *Organometallics* **2003**, *22*, 3339.
(26) Filippou, A. C.; Rohde, H.; Schnakenburg, G. *Angew. Chem., Int. Ed.* **2004**, *43*, 2243.
(27) Filippou, A. C.; Weidemann, N.; Schnakenburg, G. *Angew. Chem., Int. Ed.* **2008**, *47*, 5799.
(28) Mork, B. V.; Tilley, T. D. *Angew. Chem., Int. Ed.* **2003**, *42*, 357.
(29) Grumbine, S. D.; Chadha, R. K.; Tilley, T. D. *J. Am. Chem. Soc.* **1992**, *114*, 1518–1520.
(30) Filippou, A. C.; Weidemann, N.; Schnakenburg, G.; Rohde, H.; Philippopoulos, A. I. *Angew. Chem., Int. Ed.* **2004**, *43*, 6512.
(31) Rohde, H.; Menzel, F. R.; Filippou, A. C. *Hyperfine Interact.* **2008**, *185*, 129.
(32) Lein, M.; Szabo, A.; Kovacs, A.; Frenking, G. *Faraday Soc. Discuss.* **2003**, *124*, 365.
(33) Takagi, N.; Yamazaki, K.; Nagase, S. *Bull. Korean Chem. Soc.* **2003**, *24*, 832.
(34) Pandey, K. K.; Lein, M.; Frenking, G. *J. Am. Chem. Soc.* **2003**, *125*, 1660.
(35) Pandey, K. K.; Lledós, A. *Inorg. Chem.* **2009**, *48*, 2748.
(36) Diefenbach, A.; Bickelhaupt, M. B.; Frenking, G. *J. Am. Chem. Soc.* **2000**, *122*, 6449.
(37) Frenking, G.; Wichmann, K.; Froehlich, N.; Loschen, C.; Lein, M.; Frunzke, J.; Ravon, V. M. *Coord. Chem. Rev.* **2003**, *55*, 238.
(38) Pandey, K. K. *Coord. Chem. Rev.* **2009**, *253*, 37.
(39) Pandey, K. K.; Patidar, P.; Braunschweig, H. *Inorg. Chem.* **2010**, *49*, 6994.
(40) Pandey, K. K.; Aldridge, S. *Inorg. Chem.* **2011**, *50*, 1798.
(41) Becke, A. D. *Phys. Rev. A* **1988**, *38*, 3098.
(42) Perdew, J. P. *Phys. Rev. B* **1986**, *34*, 7406.
(43) Perdew, J. P. *Phys. Rev. B* **1986**, *33*, 8822.

(44) Snijders, J. G.; Baerends, E. J.; Vernooijs, P. *At. Data Nucl. Data Tables* **1982**, *26*, 483.
(45) Baerends, E. J.; Ellis, D. E.; Ros, P. *Chem. Phys.* **1973**, 41.
(46) Krijn, J.; Baerends, E. J. *Fit Functions in the HFS Method*; Internal Report (in Dutch); Vrije Universiteit: Amsterdam, The Netherlands, 1984.
(47) Chang, C.; Pelissier, M.; Durand, P. *Phys. Scr.* **1986**, *34*, 394.
(48) Heully, J.; Lindgren, I.; Lindroth, E.; Lundqvist, S.; Mairtensson-Pendrill, A.-M. *J. Phys. B* **1986**, *19*, 2799.
(49) van Lenthe, E.; Baerends, E. J.; Snijders, J. G. *J. Chem. Phys.* **1993**, *99*, 4597.
(50) van Lenthe, E.; van Leeuwen, R.; Baerends, E. J.; Snijders, J. G. *Int. J. Quantum Chem.* **1996**, *57*, 281.
(51) van Lenthe, E.; Baerends, E. J.; Snijders, J. G. *J. Chem. Phys.* **1996**, *105*, 6505.
(52) van Lenthe, E.; Ehlers, A. E.; Baerends, E. J. *J. Chem. Phys.* **1999**, *110*, 8943.
(53) Baerends, E. J.; Autschbach, J. A.; Berces, A.; Bo, C.; Boerrigter, P. M.; Cavallo, L.; Chong, D. P.; Deng, L.; Dickson, R. M.; Ellis, D. E.; Fan, L.; Fischer, T. H.; Fonseca Guerra, C.; van Gisbergen, S. J. A.; Groeneveld, J. A.; Gritsenko, O. V.; Grüning, M.; Harris, F. E.; van den Hoek, P.; Jacobsen, H.; van Kessel, G.; Kootstra, F.; van Lenthe, E.; Osinga, V. P.; Patchkovskii, S.; Philipsen, P. H. T.; Post, D.; Pye, C. C.; Ravenek, W.; Ros, P.; Schipper, P. R. T.; Schreckenbach, G.; Snijders, J. G.; Sola, M.; Swart, M.; Swerhone, D.; te Velde, G.; Vernooijs, P.; Versluis, L.; Visser, O.; Wezenbeek, E.; Wiesenekker, G.; Wolff, S. K.; Woo, T. K.; Ziegler, T. *ADF 2009.01*; Scientific Computing & Modelling NV: Amsterdam, The Netherlands.
(54) (a) Morokuma, K. *J. Chem. Phys.* **1971**, *55*, 1236. (b) Morokuma, K. *Acc. Chem. Res.* **1977**, *10*, 294.
(55) Ziegler, T.; Rauk, A. *Theor. Chem. Acta* **1977**, *46*, 1. (b) Zeigler, T.; Rauk, A. *Inorg. Chem.* **1979**, *18*, 1558. (c) Zeigler, T.; Rauk, A. *Inorg. Chem.* **1979**, *18*, 1755.
(56) Reed, A. E.; Curtiss, L. A.; Weinhold, F. *Chem. Rev.* **1988**, *88*, 899.
(57) Schaftenaar, G. *MOLDEN3.4*; CAOSCAMM Center: Nijmegen, The Netherlands, 1998.
(58) Wells, A. F. *Structural Inorganic Chemistry*, 5th ed.; Clarendon: Oxford, U.K., 1984.
(59) Wiberg, K. B. *Tetrahedron* **1968**, *24*, 1083.
(60) Guerra, C. F.; Handgraaf, J.-W.; Baerends, E. J.; Bickelhaupt, F. M. *J. Comput. Chem.* **2004**, *25*, 189.